UCLA
COMPUTATIONAL AND APPLIED MATHEMATICS

Image Segmentation Using Level Sets and the Piecewise-Constant Mumford-Shah Model

Tony F. Chan
Luminita A. Vese

April 2000
(revised December 2000)

CAM Report 00-14

Department of Mathematics
University of California, Los Angeles
Los Angeles, CA. 90095-1555

http://www.math.ucla.edu/applied/cam/index.html

Image segmentation using level sets and the piecewise-constant Mumford-Shah model *

Tony F. Chan and Luminita A. Vese
Department of Mathematics, University of California, Los Angeles
405 Hilgard Avenue, Los Angeles, CA 90095-1555, U.S.A.
E-mail: chan,lvese@math.ucla.edu

UCLA CAM Report 00-14, 2000

Abstract. We propose a multiphase level set algorithm for solving the minimal partition problem for image segmentation. Our starting point is the piecewise-constant Mumford-Shah model for segmentation. The proposed method can also be viewed as an extension and generalization of an active contour model without edges based on a 2-phase segmentation, developed by us earlier (Chan and Vese, 1999). Our multiphase level set formulation is new and of interest on its own: by construction, it automatically avoids the problems of vacuum and overlap; it needs only $\log n$ level set functions for n phases; it can represent boundaries with complex topologies, including triple junctions.

Keywords: energy minimization, segmentation, level sets, curvature, PDE's, denoising, edge detection, active contours, multiphase motion.

1. Introduction

The method introduced in this paper extends and generalizes the active contour model without edges based segmentation using level sets, previously proposed in (Chan and Vese, 1999). In those papers, to obtain an active contour model for object detection, the basic idea was to look for a particular partition of a given image into two regions, one representing the objects to be detected, and the second one representing the background. The active contour was given by the boundary between these two regions. It turned out that the model is a particular case of the minimal partition problem proposed (Mumford and Shah, 1989) for segmentation of images , which looks for a piecewise-constant optimal approximation, and the induced partition, of the given image. For the implementation of our earlier active contour model, the level set method of (Osher and Sethian, 1988) was successfully used, together with a particular numerical approximation, which allowed to automatically detect interior contours. The method can easily be extended to vector-valued images (Chan, Sandberg and Vese, 2000), and to several spatial

* This work has been supported in part by ONR Contract N00014-96-1-0277 and NSF Contract DMS-9973341.

dimensions, such as volumetric images (Chan and Vese, 2000), and is robust with respect to noise. In this paper, we generalize further this active contour model to segment images with more than two regions, by proposing a new variational multiphase motion by level sets for solving the minimal partition problem, as formulated by (Mumford and Shah, 1989).

Let us first give our main notations and terminology. Let $\Omega \subset I\!R^2$ be open and bounded, and let C be a set of curves in Ω. The connected components of $\Omega \setminus C$ are denoted by Ω_i, such that $\Omega = \cup_i \Omega_i \cup C$. We also denote by $|C|$ the length of curves making up C. Let $u_0 : \Omega \to I\!R$ be a bounded image-function.

The segmentation problem in computer vision, as formulated by (Mumford and Shah, 1989), can be defined as follows: given an observed image u_0, find a decomposition Ω_i of Ω, such that the new "segmented" image u varies smoothly within each Ω_i, and discontinuously across the boundaries of Ω_i.

The simplest case is obtained by restricting the segmented image u to piecewise-constant functions, i.e. u =constant c_i inside each connected component Ω_i. Then the problem is often called the "minimal" partition problem, and in order to solve it, (Mumford and Shah, 1989) proposed to minimize the following functional:

$$F^{MS}(u, C) = \sum_i \int_{\Omega_i} |u_0 - c_i|^2 dxdy + \nu|C|. \tag{1}$$

Here, ν is a positive parameter, having a scaling role. It is easy to see that, for a fixed C, this is minimized in the variables c_i by setting

$$c_i = mean(u_0) \text{ in } \Omega_i.$$

So the minimization is reduced to only with respect to the set of boundaries or curves C.

We mentioned in (Chan and Vese, 1999) that the active contour model without edges is in fact a particular case of the Mumford-Shah energy (1). It is then natural to extend our level set algorithm from (Chan and Vese, 1999) to the general case of piecewise-constant optimal approximations, and this is the main goal of the present paper. This extension should include images with triple junctions for example. When working with level sets to represent triple junctions and more than two phases, the general idea is to use more than one level set function. There are several choices for the representation of the different phases and their boundaries by level sets. A first idea was proposed in (Zhao, Chan, Merriman and Osher, 1996) (and then applied in (Samson, Blanc-Féraud, Aubert and Zerubia, 1999)): a level set function is associated to each phase or each connected component Ω_i. But then natural problems of vacuum and overlap appear. These have been solved by adding additional constraints (see (Zhao, Chan, Merriman and Osher, 1996) for more details). In this paper, we propose a different multiphase level set representation, and by definition, the distinct phases are disjoint (no overlap) and their union is the domain Ω (no vacuum); also, we need fewer level set functions to represent the same number of phases.

To summarize, in this paper we propose: (1) an extension and generalization of the previous active contour model without edges based segmentation (introduced and studied in (Chan and Vese, 1999)), to the minimal partition model (1); the proposed model can identify individual segments in images with multiple segments and junctions, as compared with the initial model (Chan and Vese, 1999), where the detected objects were belonging to the same segment; (2) we also propose a new representation for multiphase motion by level sets (requiring only $\log 2^n$ level set functions for n segments or phases), allowing triple junctions, for example. Finally, the model inherits all the advantages of the previous active contour model without edges: detection of edges with or without gradient, detection of interior contours, automatic change of topology, robustness with respect to noise. The model can perform active contours, in parallel with segmentation, denoising and edge detection.

Many other authors have studied the minimization of the Mumford-Shah functional and related problems for segmentation, both in theory and in practice. The existence of minimizers of (1) has been already proved in (Mumford and Shah, 1989); then in (Morel and Solimini, 1988), (Morel and Solimini, 1989), (Ambrosio, 1989), (Dal Maso, Morel and Solimini, 1992), for a weak formulation of the general Mumford-Shah problem. General results of existence and regularity, in any dimension, in the piecewise-constant case (1), can be found for instance in (Massari and Tamanini, 1993), (Tamanini, 1996), (Tamanini and Congedo, 1996), (Leonardi and Tamanini, 1998). Approximations to the Mumford-Shah functional have been proposed and studied in (Ambrosio and Tortorelli, 1990), (Ambrosio and Tortorelli, 1992), (March, 1992), (Chambolle, 1992), (Chambolle, 1995), (Koepfler, Lopez and Morel, 1994), (Zhu, Lee and Yuille, 1995), (Zhu and Yuille, 1996), (Shah, 1996), (Chan and Vese, 1997), (Vese and Chan, 1997), (Shah, 1999), (Chambolle and Dal Maso, 1999), (Bourdin, 1999), (Bourdin and Chambolle, 2000), and many others. In the context of image segmentation, partition and perceptual organization, we would also like to refer the reader to (Shi and Malik, 2000). Other papers related to the topic of this paper are: (Zhao, Chan, Merriman and Osher, 1996) for a variational multiphase transition model by level sets, (Samson, Blanc-Féraud, Aubert and Zerubia, 1999) for an application of the technique in (Zhao, Chan, Merriman and Osher, 1996) to image classification, (Paragios and Deriche, 1999) for a coupled geodesic active regions model for image segmentation, and (Sharon, Brandt and Basri, 2000) for a fast multiscale image segmentation; finally, we also refer the reader to (Yezzi, Tsai and Willsky, 1999) and (Yezzi, Tsai and Willsky, 2000) for related coupled curve evolution approaches for image segmentation.

For general expositions for segmentation of images by variational methods, both in theory and algorithms, we refer the reader to (Mumford, Nitzberg and Shiota, 1993) and (Morel and Solimini, 1994). Also, for an exposition of geometric PDE's and image processing (including snakes, active contours, curve evolution problems), we refer the reader to (Sapiro, 2001).

The outline of the paper is as follows: in section 2 we present the general terminology for level sets and we recall the active contour model without edges. In section 3 we present the general model for segmentation. In section 4 we validate the model on several numerical results, and we end the paper by a concluding section.

2. Preliminary notations and terminology

2.1. Review of the level set method

(Osher and Sethian, 1988) proposed an effective implicit representation of evolving curves and surfaces. Giving a curve C, as the boundary of an open set ω, we represent the curve C via the zero level set of a scalar Lipschitz function $\phi(x,y)$ (called level set function) such that

$$\begin{cases} \phi(x,y) > 0 \text{ in } \omega \\ \phi(x,y) < 0 \text{ in } \Omega \setminus \omega \\ \phi(x,y) = 0 \text{ on } \partial\omega. \end{cases}$$

(see Figure 1).

A typical example of level set function is given by the signed Euclidian distance function to the curve. Using this representation, geometrical quantities, properties and motions can be expressed. For example, using the Heaviside function $H(z)$, equal with 1 if $z \geq 0$ and with 0 if $z < 0$, the length of C and the area of ω can be expressed respectively by ((Evans and Gariepy, 1992)):

$$|C| = \int_\Omega |\nabla H(\phi)|, \quad |\omega| = \int_\Omega H(\phi) dx dy. \tag{2}$$

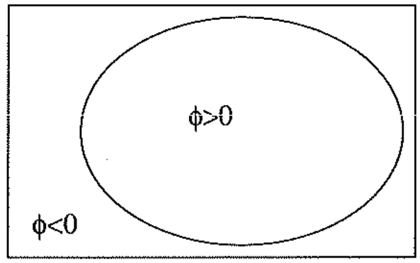

Figure 1. A curve given by a level set function ϕ, partitions the domain into two regions: $\{\phi > 0\}$ and $\{\phi < 0\}$.

We mention that the first integral is in the sense of measures.

Considering any C^1 approximation and regularization H_ε of the Heaviside function as $\varepsilon \to 0$, and denoting by $\delta_\varepsilon = H'_\varepsilon$ (an approximation to the one-dimensional Dirac delta function δ_0), we can formally write the associated Euler-Lagrange equations obtained by minimizing the above functionals with respect to ϕ, respectively:

$$\delta_\varepsilon(\phi)\mathrm{div}\Big(\frac{\nabla\phi}{|\nabla\phi|}\Big) = 0, \quad \delta_\varepsilon(\phi) = 0.$$

In (Osher and Sethian, 1988), a rescaling is made replacing $\delta_\varepsilon(\phi)$ by $|\nabla\phi|$, and the gradient descent flows are considered, giving:

$$\frac{\partial\phi}{\partial t} = |\nabla\phi|, \;\; \phi(x,y,0) = \phi_0(x,y). \tag{3}$$

(motion with constant speed, minimizing the area), and

$$\frac{\partial\phi}{\partial t} = |\nabla\phi|\mathrm{div}\Big(\frac{\nabla\phi}{|\nabla\phi|}\Big), \;\; \phi(x,y,0) = \phi_0(x,y), \tag{4}$$

(motion by mean curvature, minimizing the length).

In the previous equations, $\frac{\nabla\phi(x,y)}{|\nabla\phi(x,y)|}$ represents the unit normal to the curve at a point $(x,y) \in C$, and $\mathrm{div}\Big(\frac{\nabla\phi(x,y)}{|\nabla\phi(x,y)|}\Big)$ represents the curvature of the level curve passing through (x,y).

For more recent and general expositions on the level set method and applications, we refer the reader to (Sethian, 1999) and (Osher and Fedkiw, 2000).

2.2. Review of the active contour model without edges

We now recall the active contour model without edges from (Chan and Vese, 1999). Given the curve $C = \partial\omega$ and two unknown constants c_1

and c_2, denoting $\Omega_1 = \omega$, $\Omega_2 = \Omega \setminus \omega$, we minimize the following energy with respect to c_1, c_2 and C:

$$F_2(c_1, c_2, C) = \int_{\Omega_1=\omega} |u_0(x,y) - c_1|^2 dxdy + \int_{\Omega_2=\Omega\setminus\omega} |u_0(x,y) - c_2|^2 dxdy + \nu|C|, \tag{5}$$

or in the level set formulation, with $C = \{(x,y)|\phi(x,y) = 0\}$, (Chan and Vese, 1999):

$$F_2(c_1, c_2, \phi) = \int_{\phi>0} |u_0(x,y) - c_1|^2 dxdy + \int_{\phi<0} |u_0(x,y) - c_2|^2 dxdy + \nu|C|$$

$$= \int_\Omega |u_0(x,y) - c_1|^2 H(\phi) dxdy + \int_\Omega |u_0(x,y) - c_2|^2 (1 - H(\phi)) dxdy + \nu \int_\Omega |\nabla H(\phi)|.$$

Minimizing the energy $F_2(c_1, c_2, \phi)$ with respect to c_1 and c_2, we obtain: $c_i = mean(u_0)$ in Ω_i, for $i = 1, 2$.

Considering again H_ε and δ_ε any C^1 approximations and regularizations of the Heaviside function H and Delta function δ_0, as $\varepsilon \to 0$ and with $H'_\varepsilon = \delta_\varepsilon$, and minimizing the energy with respect to ϕ, we obtain the gradient descent flow:

$$\frac{\partial \phi}{\partial t} = \delta_\varepsilon(\phi)\Big[\nu \mathrm{div}\Big(\frac{\nabla\phi}{|\nabla\phi|}\Big) - |u_0 - c_1|^2 + |u_0 - c_2|^2\Big].$$

We also use

$$\int_\Omega |\nabla H_\varepsilon(\phi)| dxdy = \int_\Omega \delta_\varepsilon(\phi) |\nabla\phi| dxdy,$$

with $H'_\varepsilon = \delta_\varepsilon$. This model performs as active contours, looking for a 2-phase segmentation of the image. A natural generalization is introduced in the next section.

3. The description of the general model

In this section, we show how we can generalize the previous 2-phase active contour model without edges (Chan and Vese, 1999). We note that, using only one level set function, we can represent only two phases or segments in the image. Also, other geometrical features, such as triple junctions, cannot be represented using only one level set function. Our goal is to look for a multiphase level set model with which we can represent more than two segments or phases, triple junctions, and other complex topologies.

In the classical multiphase approaches by level sets, as in (Zhao, Chan, Merriman and Osher, 1996), a level set function ϕ_i is associated with each phase labeled i. A region or phase Ω_i is therefore defined by:

$$\Omega_i = \{(x,y) \in \Omega : \phi_i(x,y) \geq 0\},$$

and the boundaries between phases are defined by the union of the zero-level sets of ϕ_i, each boundary being represented twice. This formulation allows for triple junctions, for example. Again, each region or phase has its own private level set function. This function moves each level set with a normal velocity depending on the proximity to the nearest interface, thus vacuum and overlapping regions generally develop (see (Zhao, Chan, Merriman and Osher, 1996) for more details on this model). In order to prevent vacuum and overlap (i.e. to ensure Ω_i disjoint and $\cup_i \Omega_i = \Omega$), the following condition has to be always satisfied:

$$\sum_{i=1}^{n} H(\phi_i) = 1 \text{ for all } (x,y) \in \Omega,$$

which was enforced in (Zhao, Chan, Merriman and Osher, 1996) and (Samson, Blanc-Féraud, Aubert and Zerubia, 1999) as an additional term in the energy to be minimized with respect to ϕ_i, related to a Lagrange multiplier, of the form:

$$\int_\Omega (\sum_i H(\phi_i) - 1)^2 dxdy.$$

This condition has to be reinforced numerically, at each step. For problems of phase transitions for instance, where in general only a small number of phases are involved, this multiphase model is adequate and not too expensive. However, for image segmentation, we often need to represent many more phases, and then this classical approach becomes computationally expensive.

We now introduce a new multiphase level set representation in order to minimize efficiently the functional in (1), for any image u_0. We will need only $\log n$ level set functions to represent n phases or segments with complex topologies, such as triple junctions. In addition, our formulation automatically removes the problems of vacuum and overlap, because our partition is a disjoint decomposition and covering of the domain Ω by definition. This is explained next.

Let us consider $m = \log n$ level set functions $\phi_i : \Omega \to I\!R$. The union of the zero-level sets of ϕ_i will represent the edges in the segmented image. We also introduce the "vector level set function" $\Phi = (\phi_1, ..., \phi_m)$, and the "vector Heaviside function" $H(\Phi) = (H(\phi_1), ..., H(\phi_m))$ whose components are only 1 or 0. We can now define the segments or phases in the domain Ω, in the following way: two pixels (x_1, y_1) and (x_2, y_2) in Ω will belong to the same phase or class, if and only if $H(\Phi(x_1, y_1)) = H(\Phi(x_2, y_2))$. In other words, the classes or phases are given by the level sets of the function $H(\Phi)$, i.e. one class is formed by the set

$$\{(x, y)|H(\Phi(x, y)) = \text{constant vector} \in H(\Phi(\Omega))\},$$

(one phase or class contains those pixels (x, y) of Ω having the same value $H(\Phi(x, y))$).

There are up to $n = 2^m$ possibilities for the vector-values in the image of $H(\Phi)$. In this way, we can define up to $n = 2^m$ phases or classes in the domain of definition Ω. The classes defined in this way form a disjoint decomposition and covering of Ω. Therefore, each pixel $(x, y) \in \Omega$ will belong to one, and only one class, by definition, and there is no vacuum or overlap among the phases. This is an important advantage, comparing with the classical multiphase representation introduced in (Zhao, Chan, Merriman and Osher, 1996).

We label the classes by I, with $1 \leq I \leq 2^m = n$. Now, let us introduce a constant vector of averages $c = (c_1, ..., c_n)$, where $c_I = mean(u_0)$ in the class I, and the characteristic function χ_I for each class I. Then the reduced Mumford-Shah energy (1) can be written as:

$$F_n^{MS}(c, \Phi) = \sum_{1 \leq I \leq n = 2^m} \int_\Omega |u_0 - c_I|^2 \chi_I dxdy + \nu \frac{1}{2} \sum_{1 \leq I \leq n = 2^m} \int_\Omega |\nabla \chi_I|, \tag{6}$$

where the length term is given by:

$$\text{Length}(C) = \frac{1}{2} \sum_I \int_\Omega |\nabla \chi_I|,$$

where C denotes the set of edges. In order to simplify the model, we will approximate the length term by

$$\text{Length}(C) \approx \sum_i \int_\Omega |\nabla H(\phi_i)|$$

(i.e. the sum of the length of the zero-level sets of ϕ_i). Thus, in some cases, some parts of the curves will be counted more than once in the total length term, or in other words, some edges will have a different weight in the total length term. We will see that with this slight modification and simplification, we obtain very satisfactory results (it may have only a very small effect in most of the cases, because the fitting term is dominant). Also, the minimization of the Mumford-Shah energy is not optimal for image segmentation, because it only allows for triple junctions with 120^o angles, and when an edge meets the boundary of the image, it has to be only a right angle.

Therefore, the energy that we will minimize is given by:

$$F_n(c,\Phi) = \sum_{1 \leq I \leq n = 2^m} \int_\Omega |u_0 - c_I|^2 \chi_I dxdy + \sum_{1 \leq i \leq m} \nu \int_\Omega |\nabla H(\phi_i)|. \quad (7)$$

Here, the set of curves C is represented by the union of the zero level sets of the functions ϕ_i.

Clearly, for $n = 2$ (and therefore $m = 1$), we obtain the 2-phase energy (5) considered in our active contour model without edges. For the purpose of illustration, let us write the above energy for $n = 4$ phases or classes (and therefore using $m = 2$ level set functions; see Figure 2):

$$\begin{aligned} F_4(c,\Phi) &= \int_\Omega |u_0(x,y) - c_{11}|^2 H(\phi_1)H(\phi_2)dxdy \\ &+ \int_\Omega |u_0(x,y) - c_{10}|^2 H(\phi_1)(1 - H(\phi_2))dxdy \\ &+ \int_\Omega |u_0(x,y) - c_{01}|^2 (1 - H(\phi_1))H(\phi_2)dxdy \qquad (8) \\ &+ \int_\Omega |u_0(x,y) - c_{00}|^2 (1 - H(\phi_1))(1 - H(\phi_2))dxdy \\ &+ \nu \int_\Omega |\nabla H(\phi_1)| + \nu \int_\Omega |\nabla H(\phi_2)|, \end{aligned}$$

where $c = (c_{11}, c_{10}, c_{01}, c_{00})$ is a constant vector, and $\Phi = (\phi_1, \phi_2)$.

With these notations, we can express the image-function u as:

$$\begin{aligned} u &= c_{11}H(\phi_1)H(\phi_2) + c_{10}H(\phi_1)(1 - H(\phi_2)) \\ &+ c_{01}(1 - H(\phi_1))H(\phi_2) + c_{00}(1 - H(\phi_1))(1 - H(\phi_2)). \end{aligned}$$

The Euler-Lagrange equations obtained by minimizing (8) with respect to c and Φ are:

$$\begin{cases} c_{11} = mean(u_0) \text{ in } \{\phi_1 > 0, \phi_2 > 0\} \\ c_{10} = mean(u_0) \text{ in } \{\phi_1 > 0, \phi_2 < 0\} \\ c_{01} = mean(u_0) \text{ in } \{\phi_1 < 0, \phi_2 > 0\} \\ c_{00} = mean(u_0) \text{ in } \{\phi_1 < 0, \phi_2 < 0\}, \end{cases}$$

$$\begin{aligned} \frac{\partial \phi_1}{\partial t} = \delta_\varepsilon(\phi_1)\Big\{\nu \mathrm{div}\Big(\frac{\nabla \phi_1}{|\nabla \phi_1|}\Big) - \Big[\Big((u_0 - c_{11})^2 - (u_0 - c_{01})^2\Big)H(\phi_2) \\ + \Big((u_0 - c_{10})^2 - (u_0 - c_{00})^2\Big)(1 - H(\phi_2))\Big]\Big\}, \end{aligned}$$

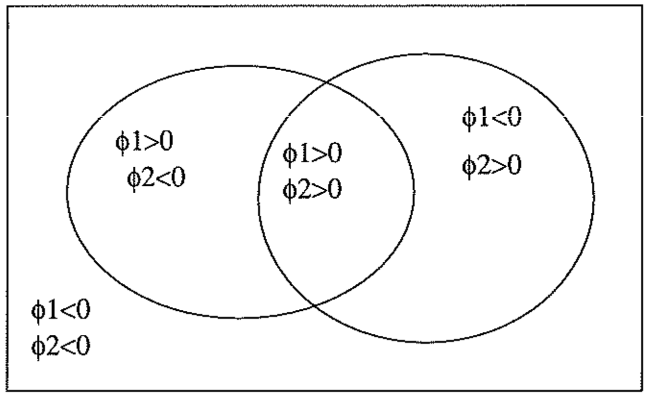

Figure 2. Two curves given by $\phi_1 = 0$ and $\phi_2 = 0$, partition the domain into four regions: $\{\phi_1 > 0, \phi_2 > 0\}$, $\{\phi_1 > 0, \phi_2 < 0\}$, $\{\phi_1 < 0, \phi_2 > 0\}$, $\{\phi_1 < 0, \phi_2 < 0\}$.

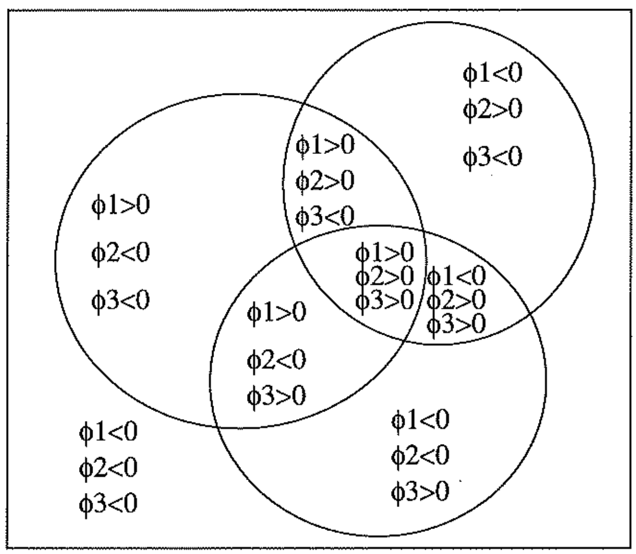

Figure 3. Three curves given by $\phi_1 = 0$, $\phi_2 = 0$, and $\phi_3 = 0$, partition the domain into eight regions: $\{\phi_1 > 0, \phi_2 > 0, \phi_3 > 0\}$, $\{\phi_1 > 0, \phi_2 > 0, \phi_3 < 0\}$, $\{\phi_1 > 0, \phi_2 < 0, \phi_3 > 0\}$, $\{\phi_1 > 0, \phi_2 < 0, \phi_3 < 0\}$, $\{\phi_1 < 0, \phi_2 > 0, \phi_3 > 0\}$, $\{\phi_1 < 0, \phi_2 > 0, \phi_3 < 0\}$, $\{\phi_1 < 0, \phi_2 < 0, \phi_3 > 0\}$, $\{\phi_1 < 0, \phi_2 < 0, \phi_3 < 0\}$.

and

$$\frac{\partial \phi_2}{\partial t} = \delta_\varepsilon(\phi_2)\Big\{\nu \mathrm{div}\Big(\frac{\nabla\phi_2}{|\nabla\phi_2|}\Big) - \Big[\Big((u_0 - c_{11})^2 - (u_0 - c_{01})^2\Big)H(\phi_1) + \Big((u_0 - c_{10})^2 - (u_0 - c_{00})^2\Big)(1 - H(\phi_1))\Big]\Big\}.$$

We note that the equations in $\Phi = (\phi_1, \phi_2)$ are governed by both mean curvature and jump of the data energy terms across the boundary.

We show in Figure 3 the partition of the domain Ω into eight regions, using three level set functions.

Remarks:

A standard procedure, as in (Zhao, Chan, Merriman and Osher, 1996), is to replace $\delta_\varepsilon(\phi_i)$ by $|\nabla\phi_i|$ in the above equations. In our numerical calculations, we keep $\delta_\varepsilon(\phi_i)$ in these equations, and we use a particular approximation of the Heaviside and Delta functions, proposed in (Chan and Vese, 1999). Our approximations for H and δ_0 are $H_\varepsilon(z) = \frac{1}{2}\left(1 + \frac{2}{\pi}\arctan\left(\frac{z}{\varepsilon}\right)\right)$, and $\delta_\varepsilon = H'_\varepsilon$, as $\varepsilon \to 0$. Using these approximations, interior contours are automatically detected.

It is easy to extend the proposed model to vector-valued functions, such as color images (following (Chan, Sandberg and Vese, 2000)). In this case, $u_0 = (u_{0,1}, ..., u_{0,N})$ is the initial data, with N channels ($N =$ 3 for color RGB images), and for each channel $i = 1, N$ we have the constants $c_I = (c_{I,1}, ..., c_{I,N})$. In this case, the model for multichannel segmentation will be:

$$F_n(c_I, \Phi) = \sum_{1 \leq I \leq n = 2^m} \sum_{i=1}^{N} \int_\Omega |u_{0,i} - c_{I,i}|^2 \chi_I dxdy + \sum_{1 \leq i \leq m} \nu \int_\Omega |\nabla H(\phi_i)|.$$

Note that, even if we work with vector-valued images, the level set functions are the same for all channels (i.e. we do not need additional level set functions for each channel). The associated Euler-Lagrange equations can easily be deduced.

This method can be extended without difficulty to higher order optimal approximations, such as piecewise-linear or piecewise-quadratic.

Finally, it is easy to show existence of minimizers for the variational problem (7). The energy $F_n(c, \Phi)$ from (7) can be expressed only function of $\chi_i = H(\phi_i)$, $1 \leq i \leq m$, which are charactersitic functions. Let's denote this energy by $\mathcal{F}_n(\chi_1, ..., \chi_m) = F_n(c(\chi_1, ..., \chi_m), \Phi)$. This is true, based on the direct methods of the calculus of variations: taking a minimizing sequence $\chi_1^k, ..., \chi_m^k$ of $\mathcal{F}_n$ ($k \to \infty$), among characteristic functions of sets of finite perimeter in Ω (i.e. with boundary of finite length), based on the lower semicontinuity of the total variation (Evans and Gariepy, 1992), we can extract a subsequence, still denoted by $\chi_1^k, ..., \chi_m^k$, such that each χ_i^k converges to χ_i strongly in $L^1(\Omega)$ (where χ_i is a characteristic function of a set of finite perimeter in Ω almost everywhere), and $\int_\Omega |\nabla\chi_i| \leq \liminf_{k\to\infty} \int_\Omega |\nabla\chi_i^k|$. Therefore, because the other (fitting) terms are continuous with respect to the $L^1(\Omega)$ topology, we deduce that $\mathcal{F}_n(\chi_1, ..., \chi_m) \leq \liminf_{k\to\infty} \mathcal{F}_n(\chi_1^k, ..., \chi_m^k)$, therefore existence of minimizers among characteristic functions $\chi_1, ..., \chi_m$ of sets of finite perimeter in Ω. From this, the constant averages c_I can easily be obtained, and the piecewise-constant image $u(x,y) = \sum_I c_I \chi_I(x,y)$, where χ_I, $1 \leq I \leq n = 2^m$, are constructed from χ_i, $1 \leq i \leq m$.

4. Experimental results

We present in this section numerical results on synthetic and real images. We will not give the details of our numerical schemes except to mention that we use the same implementation already presented in (Chan and Vese, 1999), which in particular, allows us to automatically detect interior contours. In our numerical results, we fix the space step $\triangle x = 1$, the time step $\triangle t = 0.1$, $\varepsilon = \triangle x = 1$. The only varying parameter is ν, the coefficient of the length term. We give the cpu time in seconds for our calculations, performed on a 140MHz Sun Ultra 1 with 256MB of RAM. In our numerical algorithm, we first initialize the level set functions by ϕ_i^0, then we compute the averages c_I, and we solve the PDE's in ϕ_i. Then we iterate these steps.

We show in particular that triple junctions can be represented and detected using only two level set functions, that interior contours are automatically detected and also that the model is robust in the presence of noise and complex topologies.

We first show in Figure 4 an example on a synthetic image, segmented using two level set functions with up to four phases. The image contains three objects of distinct intensities, all correctly detected and segmented. This is an improvement of our 2-phase active contour model, with which all three objects would have the same intensity in the segmented image, belonging to the same segment or phase. We also show that our model inherits all the advantages of the previous one: robust with respect to noise, automatic detection of interior contours and change of topology.

Because the energy which is minimized is not convex, and also that there is no uniqueness for the minimizers, the algorithm may not converge to a global minimizer for a given initial condition. It is then natural to consider different initial conditions for the same image with the same parameters, and to compare the steady-state solutions from our numerical algorithm. This is illustrated in Figure 5, where (a) is from Figure 4: we consider two additional initial conditions (b) and (c), and we plot the energies versus iterations (see Figure 5). For (c), we seed with small initial curves. Only using the initial conditions (a) and (c) do we compute a global minimizer for this image. For (b), the algorithm is trapped in a local minimum. For simple images, we think that some initial conditions like (a) or (b) may converge to a global minimizer. But for real images with more complicated features, we think that initial conditions of the type (c) should be used, which have the tendency to converge to a global minimizer. This type of initial condition (c) is also related to the region growing algorithm (Koepfler, Lopez and Morel, 1994). In Figure 5 we see that the energy is decreasing in all cases. We also note that using (c), the algorithm is much faster (see Figure 6).

In Figure 7 we show a noisy synthetic image with a triple junction. Using only one level set function, the triple junction cannot be represented. The classical models use three level set functions ((Zhao, Chan, Merriman and Osher, 1996) and (Samson, Blanc-Féraud, Aubert and Zerubia, 1999)). Here, we need only two level set functions to represent the triple junction. We show their zero level sets, which have to overlap on a segment of the triple junction. In Figure 8 we show another noisy image with more triple junctions, forming different angles.

In Figure 9 we show an example of a color RGB image (three channels) with contours without gradient, or cognitive contours, following (Kanizsa, 1997). We also see that this result is an improvement of the result on the same picture from (Chan, Sandberg and Vese, 2000), where the three objects had the same intensity in the end. Here, the correct intensities are detected, for each object.

We show next numerical results on two real pictures (an MRI brain image and a house), in Figures 10 and 11. We use here two level set functions, detecting four phases. We also show the final four segments detected by our algorithm. Here, we show how the model can handle complex topologies. We see in Figure 10 that the four phases identify quite well the gray matter, the white matter, etc. This is better than what the human eyes can do.

Finally, in Figure 12 we show how the model works on a color RGB image, where we use three level set functions ϕ_1, ϕ_2, ϕ_3, representing up to eight phases or colors. The algorithm detects six segments. In the classical approaches, it would have been necessarily to consider at least six level set functions. Note not all eight possible segments are present.

5. Conclusion

In this paper, we have introduced a new multiphase model for image segmentation, by variational methods and level sets. The proposed model is a common framework to perform active contours, denoising, segmentation, and edge detection. The multiphase formulation is different than the classical approaches, and has the advantage that the phases cannot produce vacuum or overlap, by construction (there is no additional constraint to prevent vacuum or overlap), and it minimizes

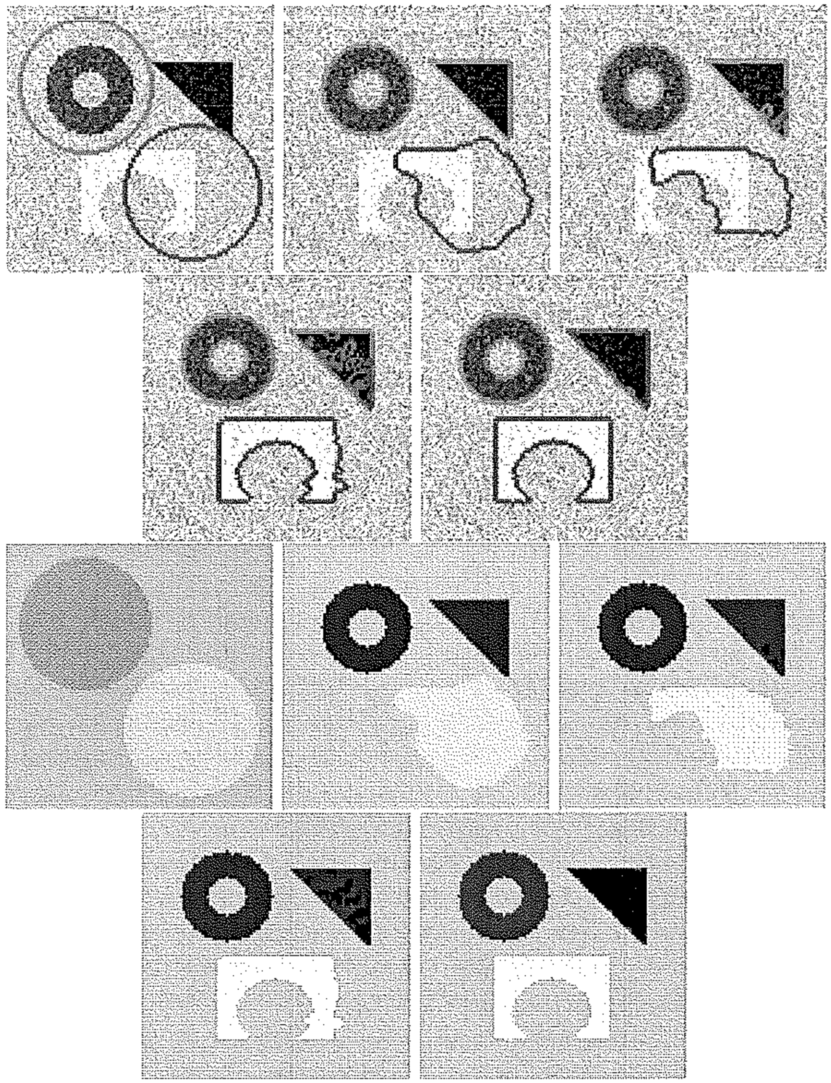

Figure 4. Segmentation of a noisy synthetic image, using two level set functions. We show from left to right and top to bottom, simulations at increasing time, as follows. First two rows: the evolving contours overlay on original image; next two rows: computed averages of the four segments $c_{11}, c_{10}, c_{01}, c_{00}$. The model detects interior contours and concave shapes automatically. $\nu = 0.0165 \cdot 255^2$, size=100x100, cpu=30.00sec.

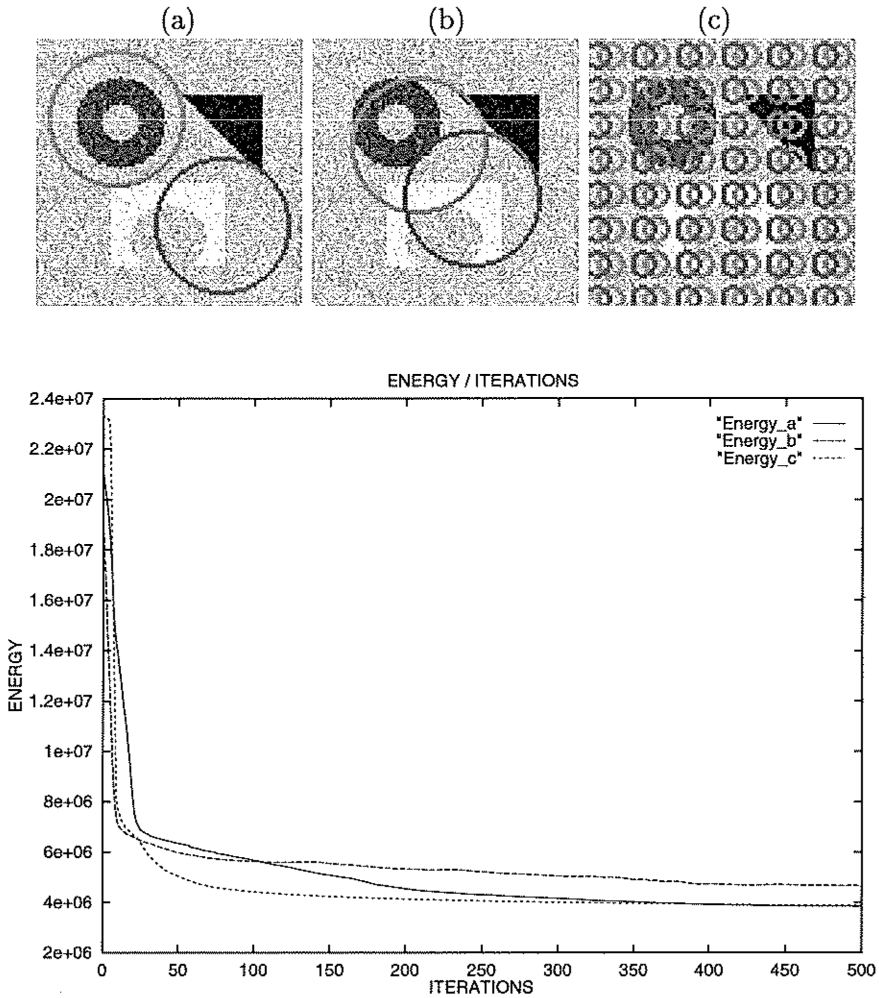

Figure 5. Three different initial conditions and the corresponding energies versus iterations.

as much as possible the computational cost, considerably reducing the number of level set functions. We show in particular that triple junctions can be represented and detected using only two level set functions. Finally, the model performs well without a priori information on the classes and their intensities. The model can be applied to other problems, such as texture segmentation and discrimination. We validated the model on various numerical results.

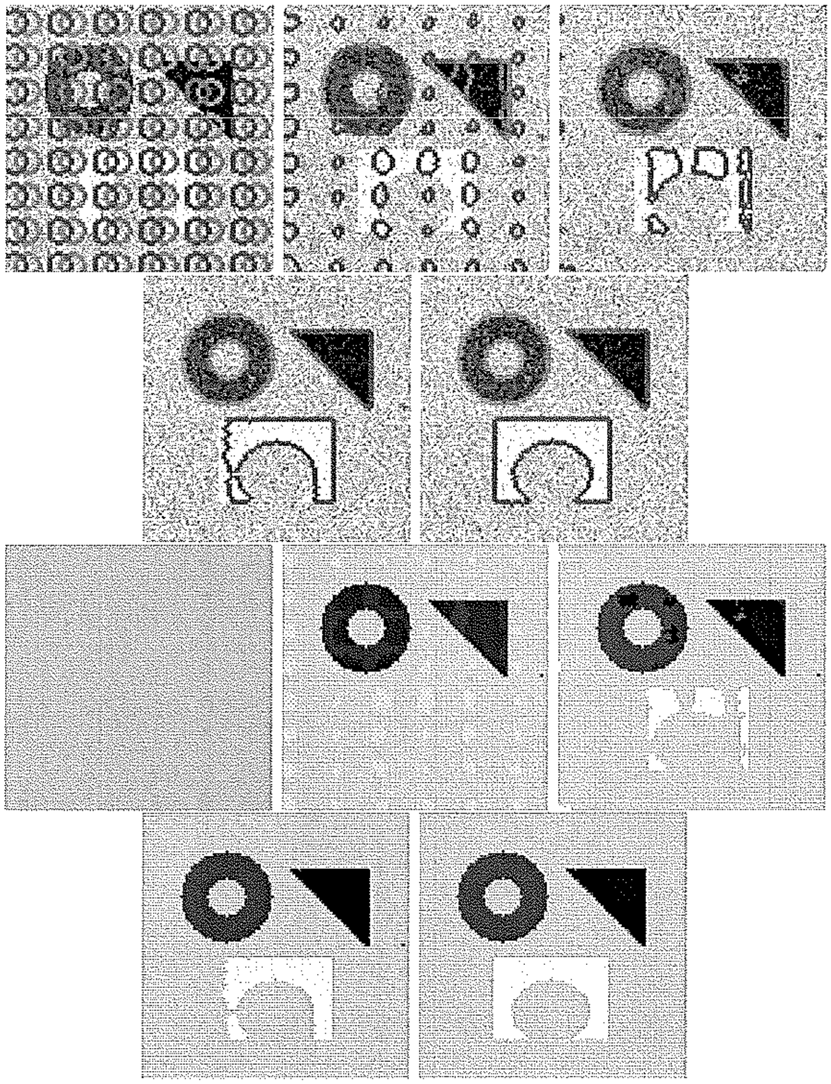

Figure 6. Results with the initial condition (c) from Fig. 5 (same parameters as in Fig. 1(a)). $\nu = 0.0165 \cdot 255^2$, size=100x100, cpu=8.46sec (very fast).

Acknowledgements

The second author would like to thank to Paul Burchard, Riccardo March and Jean-Michel Morel for very useful remarks and suggestions, and also to Gian Paolo Leonardi, for pointing us interesting references on minimal partition problems.

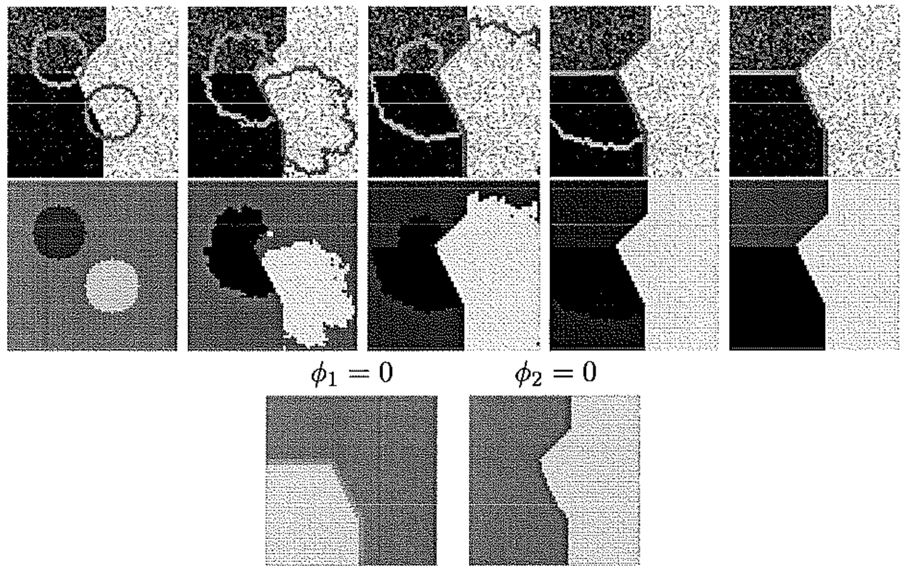

Figure 7. Results on a synthetic image, with a triple junction, using two level set functions. We also show the zero level sets of ϕ_1 and ϕ_2 (darker region: $\{\phi_i < 0\}$). $\nu = 0.05 \cdot 255^2$, size=64x64, cpu=3.51sec.

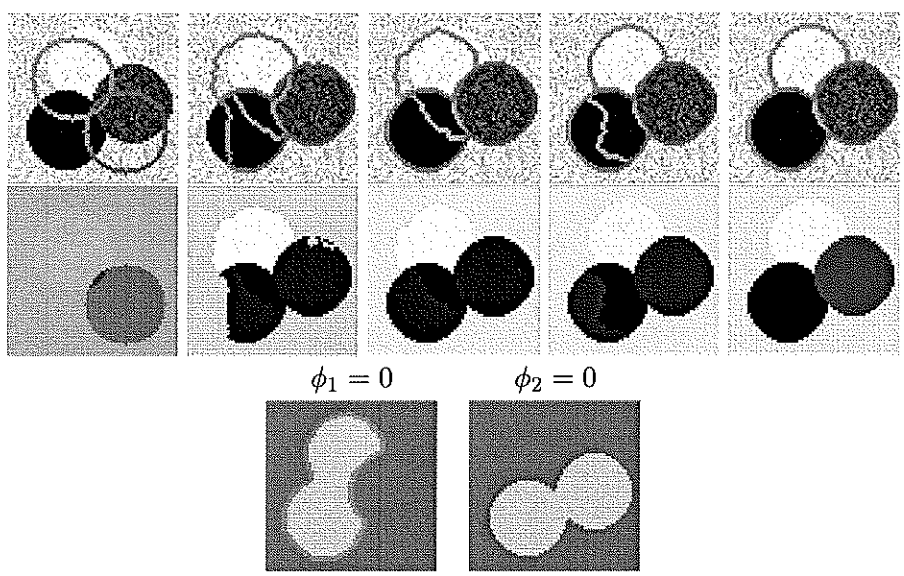

Figure 8. Results on another noisy synthetic image, containing several triple junctions. All the boundaries can be detected and represented using only two level set functions. $\nu = 0.025 \cdot 255^2$, size=64x64, cpu=11.35sec.

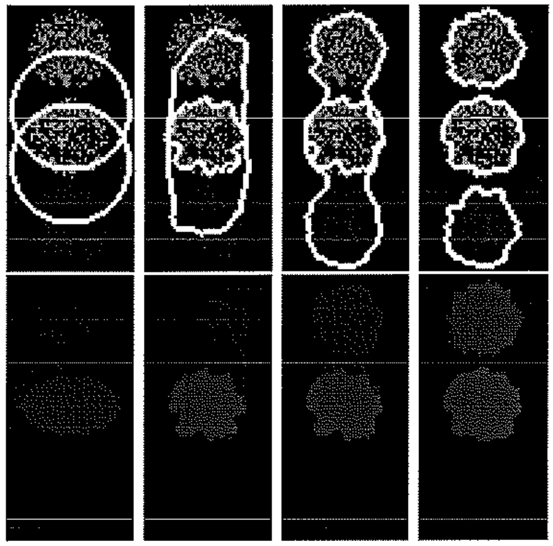

Figure 9. Numerical results on a synthetic color picture. We show in particular that contours not defined by gradient can be detected. These are called cognitive contours (Kanizsa, 1997). $\nu = 0.4 \times 255^2$, size=48x100, cpu=42.17sec.

References

Ambrosio, L. A compactness theorem for a special class of functions of bounded variation. *Boll. Un. Mat. It.*, 3(B):857–881, 1989.

Ambrosio, L. and V. M. Tortorelli. Approximation of functionals depending on jumps by elliptic functionals via Γ−convergence. *Comm. Pure Appl. Math.*, 43:999–1036, 1990.

Ambrosio, L. and V. M. Tortorelli. On the Approximation of Free Discontinuity Problems. *Bolletino U.M.I.*, 7(6-B):105–123, 1992.

Chambolle, A. Un théorème de Γ-convergence pour la segmentation des signaux. *C. R. Acad. Sci. Paris*, 314(I):191–196, 1992.

Chambolle, A. Image segmentation by variational methods: Mumford and Shah functional and the discrete approximations. *SIAM J. Appl. Math.*, 55(3):827–863, 1995.

Chambolle, A. Finite-differences discretizations of the Mumford-Shah functional. *M2AN Math. Model. Numer. Anal.*, 33(2):261–288, 1999.

Bourdin, B. Image segmentation with a finite element method. *M2AN Math. Model. Numer. Anal.*, 33(2):229–244, 1999.

Bourdin, B. and A. Chambolle. Implementation of a finite-elements approximation of the Mumford-Shah functional. *Numer. Math.*, 85(4):609–646, 2000.

Chambolle, A. and G. Dal Maso. Discrete approximation of the Mumford-Shah functional in dimension two. *M2AN Math. Model. Numer. Anal.*, 33(4):651–672, 1999.

Chan, T. and L. Vese. Variational Image Restoration & Segmentation Models and Approximations. UCLA CAM Report, 97-47, 1997.

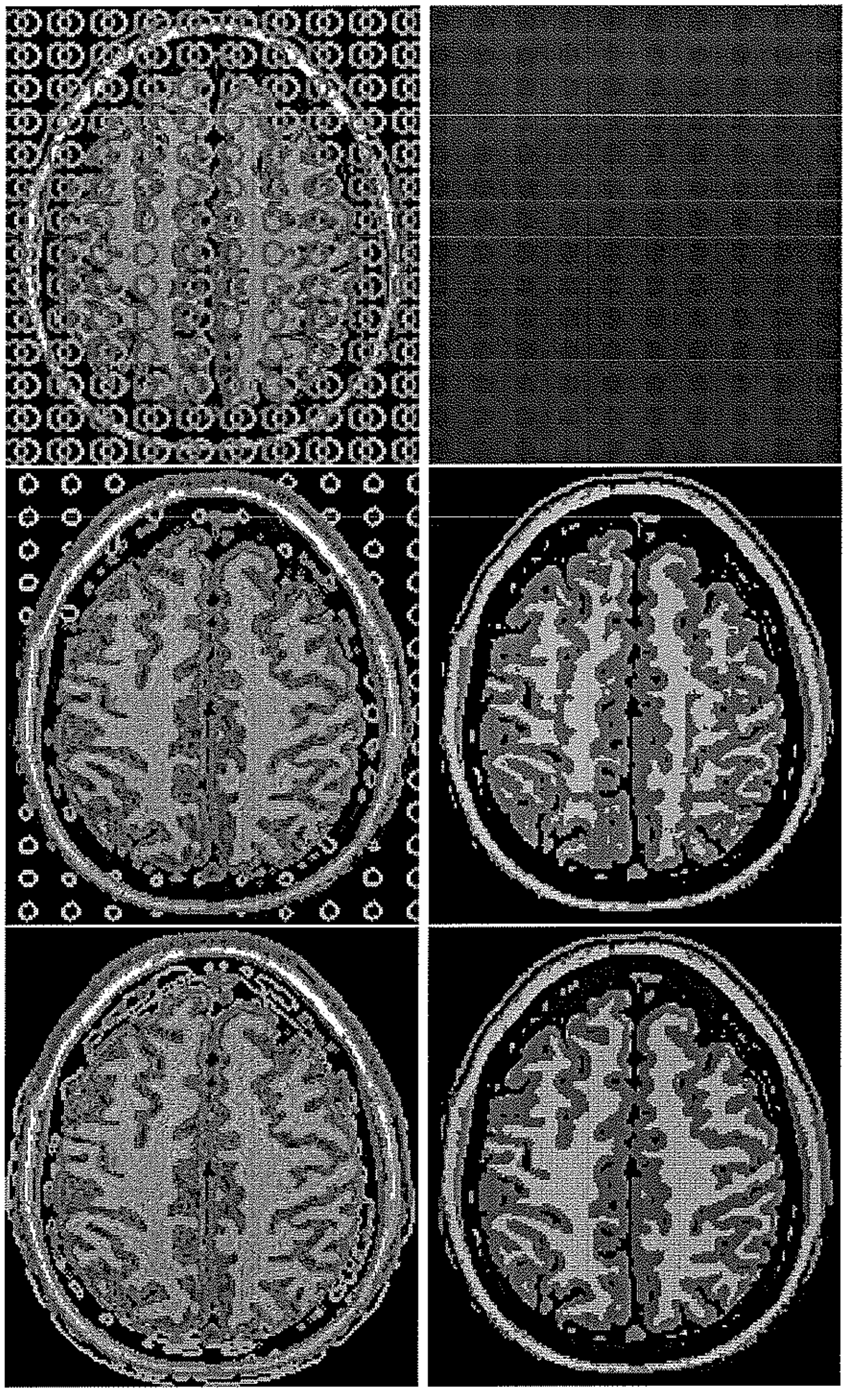

Figure 10. Segmentation of an MRI brain image, using two level set functions and four phases. $\nu = 0.01 \cdot 255^2$, size=163x181, cpu=12.86sec.

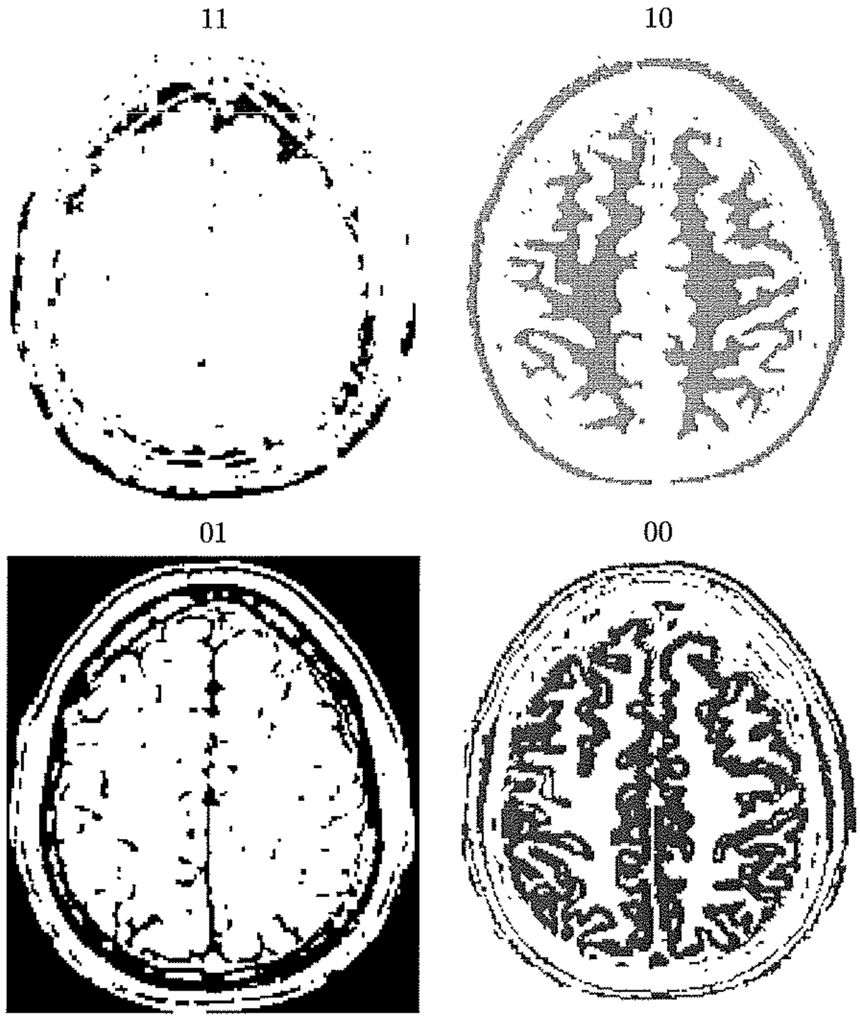

Figure 11. The algorithm depicts quite well the final four segments in the previous result (white matter, gray matter, etc.); $c_{11} = 45$, $c_{10} = 159$, $c_{01} = 9$, $c_{00} = 103$.

Chan, T. and L. Vese. Active contours without edges. UCLA CAM Report 98-53, 1999, to appear in *IEEE Transactions on Image Processing*. See also An active contour model without edges. In M. Nilsen et al., editors, *Scale-Space'99*, LNCS 1682:141–151, Springer-Verlag Berlin Heidelberg, 1999.

Chan, T. and L. Vese. Active Contours and Segmentation Models using Geometric PDE's for Medical Imaging. to appear In R. Malladi (Editor), *PDE methods with applications in bio-medical engineering*. LNCSE, Springer Verlag, 2000.

Chan, T., Sandberg, B. Y. and L. Vese. Active Contours without Edges for Vector-Valued Images. *J. of Visual Communication and Image Representation*, 11:130–141, 2000.

Figure 12. Segmentation of a real outdoor picture, using two level set functions and four phases. In the bottom row, we show the four segments obtained. The computed averages are: $c_{11} = 159$, $c_{10} = 205$, $c_{01} = 23$, and $c_{00} = 97$. $\nu = 0.01 \cdot 255^2$, size=103x89, cpu=7.88sec.

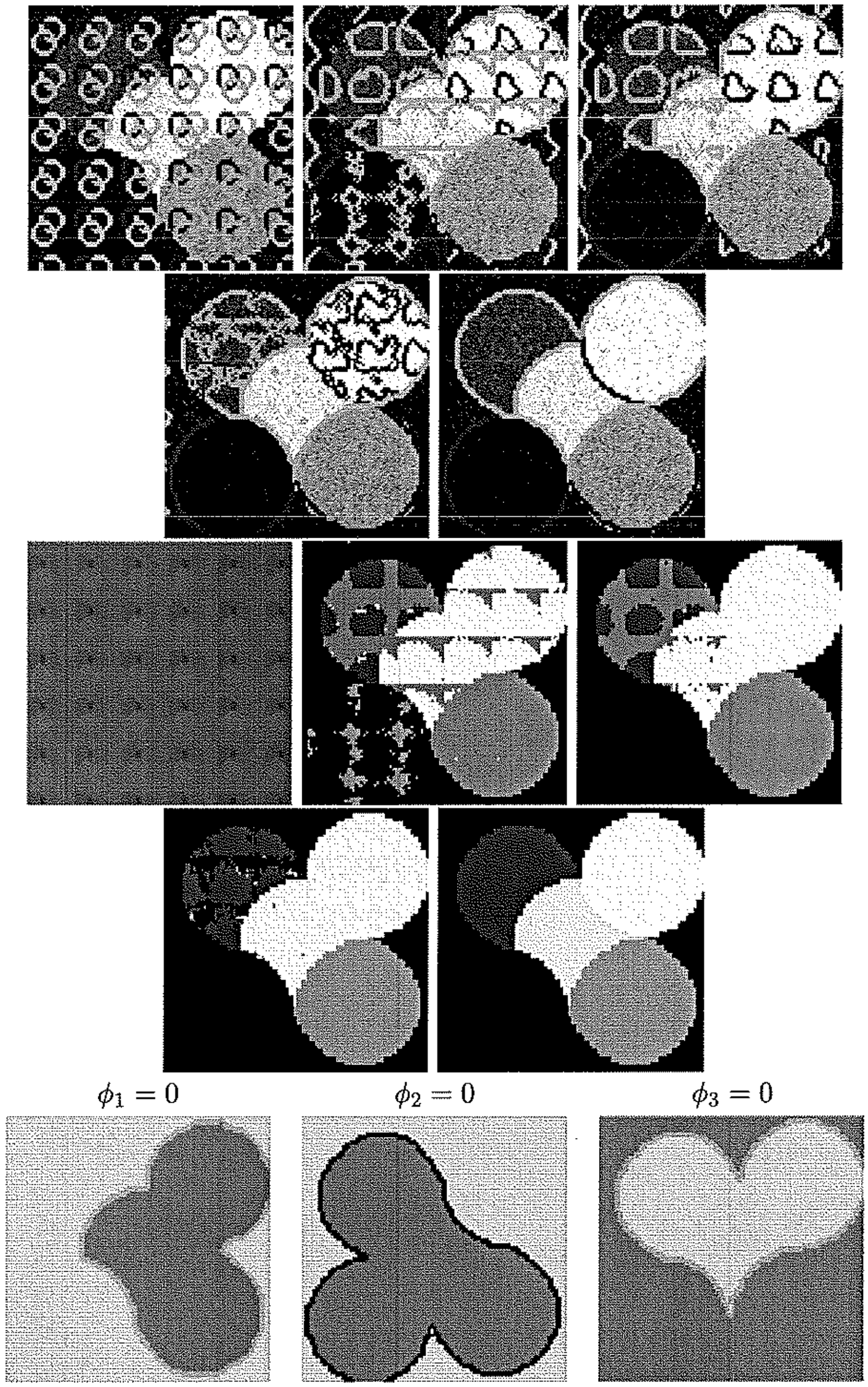

Figure 13. Color noisy picture with junctions; we use three level set functions representing up to eight regions. Here six segments are detected. We show the final zero-level sets of ϕ_1, ϕ_2, ϕ_3 (darker regions: $\phi_i < 0$). $\nu = 0.02 \cdot 255^2$, size=100x100, cpu=65.45sec.

Dal Maso, G., Morel, J. M. and S. Solimini. A variational method in image segmentation: existence and approximation results. *Acta Matematica*, 168:89-151, 1992.

Evans, L. C. and R. F. Gariepy. Measure Theory and Fine Properties of Functions. CRC Press, 1992.

Kanizsa, G. La grammaire du voir. Essais sur la perception. Diderot Editeur, Arts et Sciences, 1997.

Koepfler, G., Lopez, C. and J. M. Morel. A multiscale algorithm for image segmentation by variational method. *SIAM Journal of Numerical Analysis*, 31(1):282–299, 1994.

Leonardi, G. P. and I. Tamanini. On Minimizing Partitions with Infinitely Many Components. *Ann. Univ. Ferrara - Sez. VII - Sc. Mat.*, XLIV:41–57, 1998.

March, R. Visual Reconstruction with discontinuities using variational methods. *Image and Vision Computing*, 10:30-38, 1992.

Massari, U. and I. Tamanini. On the Finiteness of Optimal Partitions. *Ann. Univ. Ferrara - Sez. VII - Sc. Mat.*, XXXIX:167–185, 1993.

Morel, J. M. and S. Solimini. Segmentation of images by variational methods: a constructive approach. Revista Matematica Universidad Complutense de Madrid, 1:169–182, 1988.

Morel, J.M. and S. Solimini. Segmentation d'images par méthode variationnelle: une preuve constructive d'existence. *C.R. Acad. Sci. Paris Série I, Math.*, 308:465–470, 1989.

Morel, J. M. and S. Solimini. Variational Methods in Image Segmentation. Birkhäuser, PNLDE 14, 1994.

Mumford, D. and J. Shah. Optimal approximation by piecewise smooth functions and associated variational problems. *Comm. Pure Appl. Math.* 42:577–685, 1989.

Mumford, D., Nitzberg, M. and T. Shiota. Filtering, Segmentation and Depth. Springer Lecture Notes in Computer Science, Vol. 662, 1993.

Osher, S. and R. Fedkiw. Level Set Methods: An Overview and Some Recent Results. *J. Comput. Phys.*, 2000 (in press).

Osher, S. and J. A. Sethian. Fronts Propagating with Curvature-Dependent Speed: Algorithms Based on Hamilton-Jacobi Formulation. *Journal of Computational Physics*, 79:12–49, 1988.

Paragios, N. and R. Deriche. Coupled Geodesic Active Regions for image segmentation. Technical Report 3783, INRIA Sophia-Antipolis, France, 1999.

Samson, C., Blanc-Féraud, L., Aubert, G. and J. Zerubia. A Level Set Model for Image Classification. In M. Nilsen et al. (editors), *Scale-Space'99*, LNCS 1682:3060-317, Springer-Verlag Berlin Heidelberg 1999.

Sapiro, G. Geometric Partial Differential Equations and Image Analysis. Cambridge University Press, Cambridge, UK, 2001.

Sethian, J. A. Fast Marching Methods and Level Set Methods: Evolving Interfaces in Computational Geometry, Fluid Mechanics, Computer Vision and Materials Sciences. Cambridge University Press, 1999.

Shah, J. A Common Framework for Curve Evolution, Segmentation and Anisotropic Diffusion. *IEEE Conference on Computer Vision and Pattern Recognition*, June, 1996.

Shah, J. Riemannian Drums, Anisotropic Curve Evolution and Segmentation. In M. Nilsen et al. (editors), *Scale-Space'99*, LNCS 1682:129–140, Springer-Verlag Berlin Heidelberg 1999.

Sharon, E., Brandt, A. and R. Basri. Fast Multiscale Image Segmentation. *IEEE Conference on Computer Vision and Pattern Recognition*, pages 70–77, South Carolina, 2000.

Shi, J. and J. Malik. Normalized Cuts and Image Segmentation. To appear in *IEEE Transactions on Pattern Analysis and Machine Intelligence*, 2000.

Tamanini, I. Optimal Approximation by Piecewise Constant Functions. *Progress in Nonlinear Differential Equations and Their Applications*, 25:73–85, Birkhäuser Verlag, 1996.

Tamanini, I. and G. Congedo. Optimal Segmentation of Unbounded Functions. *Rend. Sem. Mat. Univ. Padova*, 95:153–174, 1996.

Vese, L. and T. Chan. Reduced Non-Convex Functional Approximations for Image Restoration & Segmentation. UCLA CAM Report, 97-56, 1997.

Yezzi, A., Tsai, A. and A. Willsky. A statistical approach to snakes for bimodal and trimodal imagery, *Int. Conf. on Computer Vision*, 1999.

Yezzi, A., Tsai, A. and A. Willsky. A fully global approach to image segmentation via coupled curve evolution equations. Submitted to *Journal of Visual Communication and Image Representation.*

Zhao, H.-K., Chan, T., Merriman, B. and S. Osher. A Variational Level Set Approach to Multiphase Motion. *J. Comput. Phys.* 127:179–195, 1996.

Zhu, S. C., Lee, T. S. and A. L. Yuille. Region competition: Unifying snakes, region growing, Energy/Bayes/MDL for multi-band image segmentation. In *Proceedings of the IEEE 5th ICCV*, pages 416–423, Cambridge, 1995.

Zhu, S. C. and A. Yuille. Region competition: Unifying snakes, region growing, and Bayes/MDL for multi-band image segmentation. *IEEE Transactions on Pattern Analysis and Machine Intelligence*, 18:884–900, 1996.